PCP
PLANT & CELL PHYSIOLOGY

Strigolactone-Based Node-to-Bud Signaling May Restrain Shoot Branching in Hybrid Aspen

Niveditha Umesh Katyayini, Päivi L.H. Rinne and Christiaan van der Schoot*

Department of Plant Sciences, Norwegian University of Life Sciences, Ås N-1432, Norway
*Corresponding author: E-mail, chris.vanderschoot@nmbu.no.
(Received April 17, 2019; Accepted August 17, 2019)

The biosynthesis and roles of strigolactones (SLs) have been investigated in herbaceous plants, but so far, their role in trees has received little attention. In this study, we analyzed the presence, spatial/temporal expression and role of SL pathway genes in *Populus tremula* × *Populus tremuloides*. In this proleptic species, axillary buds (AXBs) become para-dormant at the bud maturation point, providing an unambiguous starting point to study AXB activation. We identified previously undescribed *Populus* homologs of *DWARF27* (*D27*), *LATERAL BRANCHING OXIDOREDUCTASE* (*LBO*) and *DWARF53-like* (*D53-like*) and analyzed the relative expression of all SL pathway genes in root tips and shoot tissues. We found that, although AXBs expressed *MORE AXILLARY GROWTH1* (*MAX1*) and *LBO*, they did not express *MAX3* and *MAX4*, whereas nodal bark expressed high levels of all SL biosynthesis genes. By contrast, expression of the SL perception and signaling genes *MAX2*, *D14* and *D53* was high in AXBs relative to nodal bark and roots. This suggests that AXBs are reliant on the associated nodes for the import of SLs and SL precursors. Activation of AXBs was initiated by decapitation and single-node isolation. This rapidly down-regulated SL pathway genes downstream of *MAX4*, although later these genes were upregulated coincidently with primordia formation. GR24-feeding counteracted all activation-related changes in SL gene expression but did not prevent AXB outgrowth showing that SL is ineffective once AXBs are activated. The results indicate that nodes rather than roots supply SLs and its precursors to AXBs, and that SLs may restrain embryonic shoot elongation during AXB formation and para-dormancy in intact plants.

Keywords: Axillary bud • DWARF27 (D27) • DWARF53-like (D53-like) • LATERAL BRANCHING OXIDOREDUCTASE (LBO) • *Populus*.

Introduction

In deciduous trees, crown architecture arises through the coordinated action of terminal and axillary meristems (AXMs). In contrast to annuals, like *Arabidopsis* (Grbić and Bleecker 2000, Long and Barton 2000, Greb et al. 2003), the AXMs of deciduous trees arise in the axils of emerging leaves and produce axillary buds (AXBs) with bud scales (Garrison 1955). The timing and pattern of branch formation reflect different branching styles. In sylleptic branching, newly formed AXBs produce branches in the same season, whereas in proleptic branching they may produce them only in the following seasons (Hallé et al. 1978, Ceulemans et al. 1990, Wu and Stettler 1998, Barthélémy and Caraglio 2007). The sylleptic branching pattern is strongly influenced by the prevailing environmental conditions, revealing considerable plasticity in architectural design. On the other hand, in proleptic species AXB outgrowth is postponed to the next growing season, resulting in a more robust branching pattern (Cline 1997).

Hybrid aspen (*Populus tremula* × *Populus tremuloides*, clone T89) is a typical proleptic species. AXBs develop during the growing season until the dwarfed side shoot, enclosed by five scales, has produced about 10 embryonic leaves. This point is referred to as the bud maturation point (BMP; Rinne et al. 2015). These mature AXBs partially dehydrate and remain para-dormant, at least until the next growing season, but they can be activated expeditiously by decapitation. This allows the investigation of processes that exclusively relate to AXB activation, and not to AXB formation. In sylleptic tree species, where branches are initiated in the same season, such unambiguous starting point is lacking.

In woody perennials, very little is known about the molecular processes that control branching. By contrast, these processes are under intensive investigation in herbaceous annuals, like *Arabidopsis* and pea, as well as in the monocot rice (Sorefan et al. 2003, Domagalska and Leyser 2011, Wang and Li 2011). They show that the AXB activation is regulated by a network of interacting hormones. Although auxin and cytokinins are the classic branching hormones (King and Van Staden 1988, Müller and Leyser 2011), recent work with woody species shows that gibberellins (GA) also play a role (Ni et al. 2015, Rinne et al. 2016). Crucial newcomers in this network are carotenoid-derived terpenoid lactones, referred to as strigolactones (SLs) that suppress branching (Gomez-Roldan et al. 2008, Umehara et al. 2008, Ferguson and Beveridge 2009).

So far, all natural SLs have been isolated from root exudates and identified based on their capacity to stimulate germination of parasitic plant seeds (Kobae et al. 2018). The first SL, identified in root exudates of cotton, was named strigol because it stimulated the germination of witchweed (*Striga lutea* Lour) seeds (Cook et al. 1966, Cook et al. 1972). When *Striga* seeds are in close proximity of the roots of a strigol exuding host plant, they will germinate and parasitize the plant. The finding

Plant Cell Physiol. 60(12): 2797–2811 (2019) doi:10.1093/pcp/pcz170, Advance Access publication on 26 August 2019, available online at https://academic.oup.com/pcp

that not only host plants but also non-hosts like cotton exuded SL-like compounds to the rhizosphere, indicated that SLs had some distinct function unrelated to parasitic seed germination (Wang and Bouwmeester 2018). Such non-host SL exudation was found to attract arbuscular mycorrhizal (AM) fungi to colonize plant roots, particularly under conditions of phosphate starvation (Yoneyama et al. 2007, López-Ráez et al. 2008, Carbonnel and Gutjahr 2014). In an established symbiotic relationship, the AM fungi deliver phosphate to the plant, while in return the plant provides sugars (Akiyama et al. 2005, Besserer et al. 2006).

In addition to inhibiting shoot branching and attracting AM fungi, SLs have crucial roles in secondary growth, root development and leaf senescence (Gomez-Roldan et al. 2008, Umehara et al. 2008, Kapulnik et al. 2011, Rasmussen et al. 2012, Yamada et al. 2014). The role of SL in shoot branching has been analyzed in branching mutants of *Arabidopsis* (Sorefan et al. 2003, Booker et al. 2004, Booker et al. 2005, Domagalska and Leyser 2011, Seto and Yamaguchi 2014), pea (Beveridge et al. 1997, Hamiaux et al. 2012), petunia (Drummond et al. 2009, Hamiaux et al. 2012) and rice (Wang and Li 2011, Zhang et al. 2014).

A generalized SL pathway can be subdivided into three distinct parts, which are spatially separate: the plastid, the cytoplasm/symplasm and the nuclei of cells in the target areas (**Fig. 1**). In the plastid carotenoid pathway (Matusova et al. 2005), all-*trans*-β-carotene is converted to the biosynthetic intermediate carlactone (CL), which is exported to the cytoplasm (Alder et al. 2012, Kobae et al. 2018, Yoneyama et al. 2018). CL biosynthesis involves three important classes of plastid enzymes. In *Arabidopsis*, these include the isomerase DWARF27 (D27), and two carotenoid cleavage dioxygenases (CCD7 and CCD8), encoded by *MORE AXILLARY GROWTH3* (*MAX3*) and *MORE AXILLARY GROWTH4* (*MAX4*), respectively.

CL is a chemically stable and graft-transmissible intermediate that must be converted by the ER-anchored enzyme MORE AXILLARY GROWTH1 (MAX1; Cytochrome P450) to carlactonoic acid (CLA; Abe et al. 2014) or 4-deoxyorobanchol (4DO; Alder et al. 2012). CL and CLA are non-canonical SLs that possess the essential enol ether-D-ring moiety required for biological activity (Zwanenburg et al. 2009) but not the complete ABCD ring system found in canonical SLs (Yoneyama et al. 2018). CLA, the universal precursor of a variety of species-dependent SLs (Iseki et al. 2018), is methylated to methyl carlactonoate (MeCLA) in roots and shoots by an unidentified enzyme (Abe et al. 2014, Iseki et al. 2018, Yoneyama et al. 2018). In *Arabidopsis*, MeCLA is a substrate of the 2-oxoglutarate-dependent dioxygenase LATERAL BRANCHING OXIDOREDUCTASE (LBO), which oxidizes MeCLA to a compound referred to as MeCLA+16D (Brewer et al. 2016).

SL perception requires the F-box protein MAX2 and the unconventional hormone receptor DWARF14 (D14), a protein of the α/β-fold hydrolase superfamily. In *Arabidopsis*, as well as rice, SL triggers interactions among D14, MAX2 and SMXL/D53 in the nuclei of target cells (Zhou et al. 2013, Zhao et al. 2015, Liang et al. 2016, Yao et al. 2016). In rice, the D53 protein was identified as a repressor of the SL signaling pathway, which is targeted for degradation after SL treatment (Jiang et al. 2013).

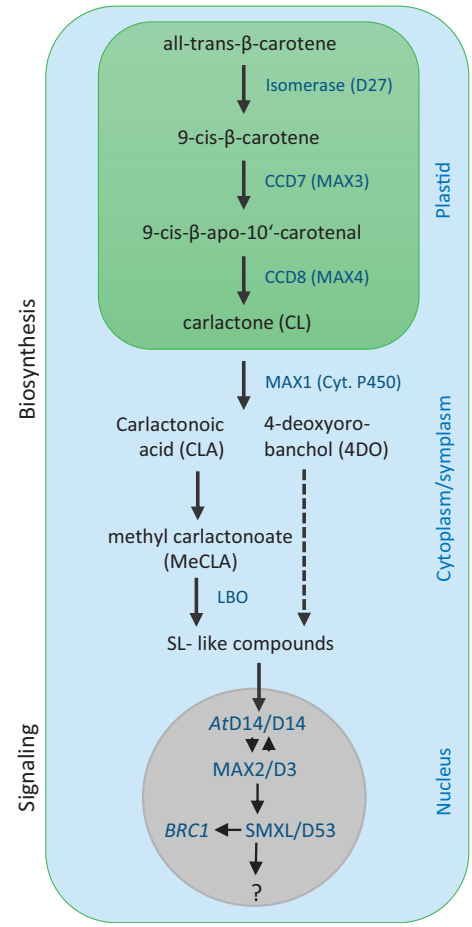

Fig. 1 Generalized scheme of SL biosynthesis and signaling. The schema envisions three compartments: the biosynthetic compartment of the plastid (green) where CL is produced, the cytoplasmic and the symplasmic compartment (light blue) where excreted CL is converted to CLA/4DO by MAX1, and the nucleus (grey) where perception occurs. CLA is converted to MeCLA, and further by LBO. The SL-like compounds downstream of MeCLA and 4DO (stippled line) are imported into the nuclei of target cells, where *At*D14/D14 interacts with the F-box protein MAX2/D3 in an SL-dependent manner to ubiquitinate and degrade the transcription repressor SMXL/D53, resulting in expression of *BRC1*.

The rice F-box protein DWARF3 (D3, ortholog of *Arabidopsis* MAX2) plays a crucial role in mediating this degradation. It requires D14 to ubiquitinate D53 for degradation by the D14-SCF^{D3} ubiquitin ligase, to promote SL signaling and responses (Jiang et al. 2013, Zhou et al. 2013). A downstream target of SL signaling is the gene *BRANCHED1* (*BRC1*)/*TEOSINTE BRANCHED1* (*TB1*), which encodes a transcription factor that suppresses shoot branching (Doebley et al. 1997, Aguilar-Martínez et al. 2007, Finlayson 2007, Finlayson et al. 2010, Seale et al. 2017).

Although in annuals SL biosynthesis and signaling genes are largely conserved (Yao et al. 2018), in woody perennials their presence and function remain mostly unexplored. Given the distinct initiation, development and composition of AXBs in hybrid aspen (Rinne et al. 2015), it is uncertain if the complete pathway is present and functionally conserved in *Populus*. So far, few SL pathway genes have been identified in perennials

(Wang and Li 2006, Czarnecki et al. 2014, Zheng et al. 2016). However, it has been reported that *Populus* root exudate contains 4DO, a canonical SL, and the non-canonical SLs CLA and MeCLA (Xie 2016). Tentative evidence indicates that the inhibition of shoot branching is mediated by non-canonical SLs (Yoneyama et al. 2018). Indeed, grafting experiments with pea, *Arabidopsis* and petunia showed that root-produced CL can be imported by the shoot (Beveridge et al. 2000, Morris et al. 2001, Turnbull et al. 2002). However, to inhibit branching in *Arabidopsis* it must be converted by MAX1 to CLA, as CL is ineffective in *max1* mutants (Scaffidi et al. 2013). In addition, these studies showed that SL biosynthesis genes can also be expressed in shoots, as a wild type scion on an SL-deficient mutant stock does not display a branching phenotype. However, so far SL-like compounds have not been isolated from shoots, indicating that their levels may be very low (Kobae et al. 2018).

In AXBs of hybrid aspen, two *MAX1* orthologs and two orthologs of the SL target gene *BRC1* are expressed (Rinne et al. 2015). All four genes were upregulated during AXB development, reaching their highest levels in mature AXBs, whereas decapitation at the BMP downregulated them in the proximal AXBs (Rinne et al. 2015). In agreement with this, in *Populus* × *canescens*, knockdown of SL biosynthesis genes reduced *BRC1* expression and induced branching, like knockdown of *BRC1* and *BRC2* (Muhr et al. 2016, Muhr et al. 2018). Together, these findings suggest that at least part of the SL biosynthesis and signaling genes as well as downstream targets are functional in *Populus*.

Our first aim was to investigate whether close homologs of the *Arabidopsis* and rice SL pathway genes (**Fig. 1**) were present in the *Populus trichocarpa* genome (Tuskan et al. 2006), and if and where they were expressed in hybrid aspen. In addition, we aimed to assess whether the unique lifestyle of woody perennials and their complicated bud structure would put different demands on the spatial layout of the SL biosynthesis and signaling paths. Here, we, identified all SL pathway genes in the *P. trichocarpa* genome, and analyzed their expression in roots and shoot tissues of the non-branching hybrid aspen seedlings (**Fig. 2**). Nodal bark, rather than root tips, appeared to be major hubs for SL biosynthesis, whereas the AXBs were dominant centers of SL perception. Decapitation-activated AXBs rapidly downregulated SL pathway genes coincident with the start of embryonic shoot (ES) elongation, suggesting that SL inhibits this elongation in intact plants.

Results

Expression of SL biosynthesis genes in hybrid aspen

The first enzyme in the SL biosynthesis pathway is isomerase D27 (**Fig. 1**), but so far it has not been reported for woody perennials. We identified three close homologs of the *Oryza sativa D27* gene (Lin et al. 2009) in the *P. trichocarpa* genome (Supplementary Fig. S1), and named them *D27a*, *D27b* and *D27c*. Transcripts of *D27a* and *D27c* were expressed in most plant parts, whereas *D27b* was undetectable. *D27a* transcript levels were higher than those of *D27c*, in the apex and particularly in the sink and source leaves (**Fig. 3A**). Remarkably, in roots, thought to be the major source of SL, *D27a* transcripts were undetectable, and *D27c* expression was also very low (**Fig. 3A**). However, roots expressed *MAX3* and *MAX4*, the two downstream SL biosynthesis genes that mediate CL production (**Figs. 1**, **3B**). By contrast, the expression of *MAX3* and *MAX4* was virtually absent in developing and mature AXBs, but surprisingly the associated nodes expressed both genes at high levels (**Fig. 3B**). The expression of *MAX3* was higher than that of *MAX4* in both sink and source nodes. The sink nodes, which support the young developing AXBs, expressed both genes at very high levels (**Fig. 3B**, inset). *MAX1* genes were expressed in all plant parts, including the AXBs (**Fig. 3C**). However, because the AXBs themselves did not express *MAX3* and *MAX4*, *MAX1* must serve to convert imported CL. As the expression of *MAX3* in both sink and source nodes, and *MAX4* in sink nodes, were at exceptionally high levels compared to roots (**Fig. 3B**), the AXBs of hybrid aspen are likely to import CL from the nodes rather than from the roots.

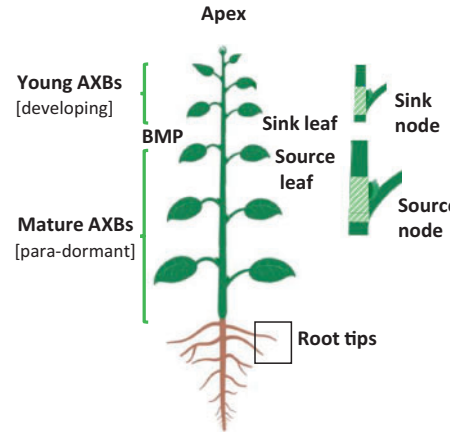

Fig. 2 Cartoon depicting the position of young and mature AXBs. The developing young AXBs become para-dormant at the BMP. Sink node and source node denote bark tissue, isolated from the nodes of young and mature AXBs, respectively (hatch pattern). Root material was isolated exclusively from root tips.

In *Arabidopsis*, a downstream product of CLA is the methyl ester MeCLA (**Fig. 1**), which can directly interact with the SL signaling component D14 (Abe et al. 2014). However, MeCLA is also substrate for LBO (**Fig. 1**), and conversion into other SL-like compounds might be required for at least some of its bioactivity (Brewer et al. 2016). To date, no information is available about its precise role, and whether it is conserved in woody species.

To identify the *LBO* gene, we searched the *P. trichocarpa* genome for a putative ortholog of *AtLBO* (encoded by locus *At3g21420*) and identified a protein encoded by Potri.010G023600 as *PtLBO*. The number of amino acids in *PtLBO* (364 aa) is identical to that in *AtLBO* (Supplementary Fig. S2) and exhibits 84% similarity and 66% identity at the

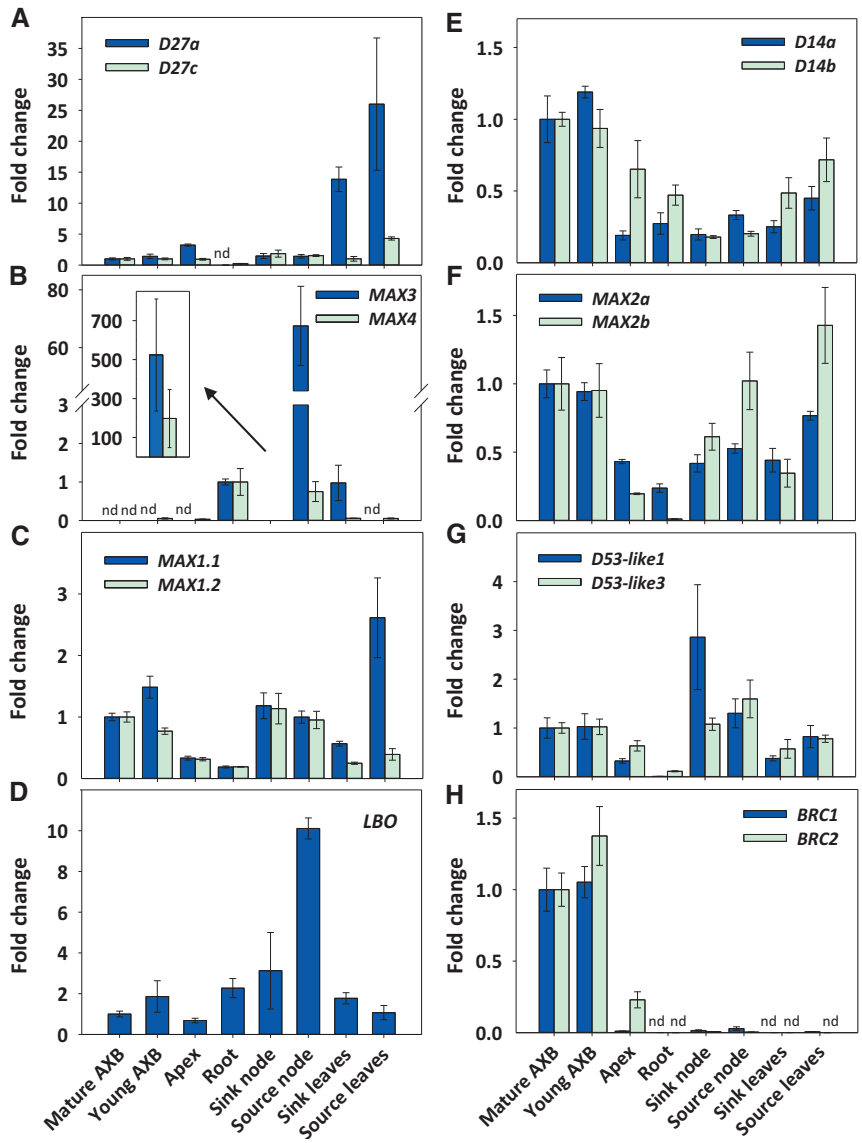

Fig. 3 Expression of SL biosynthesis genes in different plant parts. Expression (fold change) was analyzed in mature AXBs, young AXBs, apex, root, sink node, source node, sink leaves and source leaves. (A) *D27a* and *D27c*. (B) *MAX3* and *MAX4*. (C) *MAX1.1* and *MAX1.2*. (D) *LBO*. (E) *D14a* and *D14b*. (F) *MAX2a* and *MAX2b*. (G) *D53-like1* and *D53-like3*. (H) *BRC1* and *BRC2*. Values represent the means of three biological replicates ±SE ($n = 6$ plants). nd, not detected. The expression value of the mature AXBs or roots was set at 1.

amino acid level. *LBO* was expressed throughout the plant, including AXBs, but the highest relative expression was found in source nodes, followed by sink nodes and roots (Fig. 3D).

Expression of SL signaling genes in hybrid aspen

In *Arabidopsis*, the α/β-hydrolase D14 and the F-box protein MAX2 are essential components in the SL-dependent suppression of AXB outgrowth. D14, thereby, functions as an SL receptor with catalytic activity. Although D14 is localized in the cytoplasm and nucleus (Chevalier et al. 2014), the nuclear pool is responsible for D14 function (Liang et al. 2016). SL triggers the physical interaction among nuclear-localized D14, MAX2 and SMXL7/D53 in the nuclei of target cells, resulting in degradation of SMXL7/D53 (Liang et al. 2016). *D14* as well as *MAX2* homologs have been identified previously in a *Populus* species (Czarnecki et al. 2014, Zheng et al. 2016), but their tissue-specific expression and role in AXBs have not been investigated. The present data show that in hybrid aspen all plant parts expressed *D14a* and *D14b*. Transcript levels in AXBs were two to three times higher than in roots, while levels in the corresponding nodes were somewhat lower than in roots (Fig. 3E). A similar trend was found for *MAX2a* and *MAX2b* transcripts, although here the lowest expression level was in roots instead of nodes (Fig. 3F). The relative expression of both signaling genes, *MAX2* and *D14*, was highest in AXBs. However, *MAX2b* was also well expressed in source tissues (Fig. 3E, F). Thus, although the production of SL-like compounds downstream of CL occurs predominantly in both sink and source nodes, SL perception appears particularly dominant in AXBs (Fig. 3E–G).

Downstream targets of SL signaling in hybrid aspen

In rice, enhanced SL signaling results in the proteasomal degradation of the *Os*D53 (Fig. 1), a suppressor of SL signaling, resulting in inhibition of AXB activation and outgrowth (Jiang et al. 2013, Zhou et al. 2013). Using phylogenetic analysis, we identified three *P. trichocarpa* homologs of *OsD53*, which we named *D53-like1*, *D53-like2* and *D53-like3* (Supplementary Fig. S6). All three genes were expressed throughout the plant, with the possible exception of roots in the case of *D53-like1* and *D53-like2* (Fig. 3G; Supplementary Fig. S3A). As *D53-like2* was unresponsive to decapitation, we considered it not relevant for branching (Supplementary Fig. S3B). Although hardly expressed in roots, AXBs and their associated nodes expressed *D53-like1* and *D53-like3* at appreciable levels (Fig. 3G). Expression in the apex was about half of that in AXBs and nodes.

Among the downstream targets of SL in *Arabidopsis* is the branch-inhibitor gene *BRC1* (Fig. 1), which encodes a class II TB1 CYCLOIDEA PCF (TCP) type transcription factor (Aguilar-Martínez et al. 2007, Finlayson 2007) that represses cell proliferation (Schommer et al. 2014). As we showed previously, hybrid aspen has two *BRC* genes, *BRC1* and *BRC2*, which are upregulated in developing AXBs (Rinne et al. 2015). Here, we confirm that *BRC1* and *BRC2* are highly expressed in AXBs, but that their relative expression elsewhere in the plant was very low or undetectable, except for *BRC2* in the shoot apex (Fig. 3H). This suggests that SL signaling targets *BRC1* and *BRC2* in the dwarfed side shoots of the AXBs to inhibit outgrowth.

Decapitation-induced developmental changes in AXBs

To assess the role of SL biosynthesis and signaling in the activation of mature, developmentally inactive AXBs, plants were decapitated at the BMP. Changes in gene expression were analyzed in the AXB proximal to the decapitation point. To provide context to these gene expression changes, we investigated the time-frame of decapitation-induced developmental changes in the proximal AXB (Fig. 4). The lengths of the AXBs and ESs were measured, and the number of embryonic leaves counted at regular intervals post decapitation (Fig. 4B). The length of the proximal AXB increased gradually after decapitation, and the increase was statistically significant after 48 h. The elongation of the ES shoot followed a similar pattern, albeit a statically significant increase occurred 1 d earlier (Fig. 4B). The number of embryonic leaves was constant over the entire 96-h period, showing that no neo-formed leaves were produced (Fig. 4B). Together, the data show that decapitation-induced changes in gene expression during the first 48 h clearly relate to elongation of the ES stem, and not to the formation of new leaves at the shoot apical meristem (SAM) of the ES.

Post-decapitation expression of SL biosynthesis and signaling genes

To pinpoint the role of SL biosynthesis and signaling in the early activation events of the proximal, mature AXBs, we restricted our analyses to the genes that were expressed in the AXBs themselves (Fig. 3). The expression of *D27*, *MAX1*, *LBO*, *D14*, *MAX2* and *D53-like* genes, as well as the downstream target genes *BRC1* and *BRC2*, was analyzed in AXBs during the critical 0–48 h post-decapitation period (Fig. 5).

The expression of *D27a* and *D27c* was somewhat reduced between 6 and 12 h after decapitation, and thereafter gradually recovered (Fig. 5A), although these changes were not statistically significant. As *MAX3* and *MAX4* were not expressed in AXBs of intact plants (Fig. 3B), the modest decapitation-induced alterations in the two *D27* genes might not relate SL-mediated events in the AXBs. *MAX1.1* and *MAX1.2* expressions, and putative CLA production, were significantly reduced by decapitation between 2 and 6 h (Fig. 5B). *LBO* expression showed a statistically significant increase that started between 12 and 24 h (Fig. 5C).

Although *D14a* and *D14b* were specifically expressed at high levels in all AXBs of intact plants (Fig. 3E), decapitation significantly reduced transcript levels in the AXB proximal to the decapitation point (Fig. 5D). The transcript levels of both *D14* genes declined significantly between 2 and 6 h, and onward. Although *D14b* expression diminished more gradually, both *D14* genes had the same low level at the 48 h time point (Fig. 5D). The expression of F-box genes *MAX2a* and *MAX2b* also decreased relatively early, between 2 and 6 h post decapitation, although *MAX2a* expression tended to recover (Fig. 5E). Of the two *D53-like* genes, *D53-like1* expression was significantly reduced by decapitation between 0 and 2 h. By contrast, the decrease in *D53-like3* expression was only transient, and it increased significantly between 12 and 24 h (Fig. 5F).

The downstream target of SL signaling, *BRC1*, which was highly expressed in mature AXBs of intact plants (Fig. 3H), was rapidly and strongly downregulated after decapitation between 0 and 2 h in the proximal AXB. *BRC2* expression was more gradually and modestly reduced (Fig. 5G).

Taken together, the downregulation of *MAX1.1*, *MAX1.2*, *D14a*, *D14b*, *MAX2b*, *D53-like1*, *BRC1* and *BRC2* as well as the upregulation of *LBO* (Fig. 5) preceded the initial phase of ES stem elongation, and the subsequent neo-formation of leaves (Fig. 4).

Developmental changes in AXBs of GR24-treated single-node systems

As we found that SL pathway dynamics within the AXB-node complex reflected the transition from inactivity to activation, we hypothesized that an increase in SL content will prevent AXB activation. To investigate the effect of SL application, we used single-node systems to xylem-feed the SL analog GR24 into AXBs (Fig. 6). These systems, commonly used to study bud burst (Rinne et al. 2011, Brewer et al. 2015, Rinne et al. 2016, Seale et al. 2017, Xie et al. 2017), are particularly useful in woody perennials where direct application to the buds is ineffective. Xylem-feeding also enables the investigation of AXB activation independent from the constraints of apical dominance and leaf- or root-derived signals.

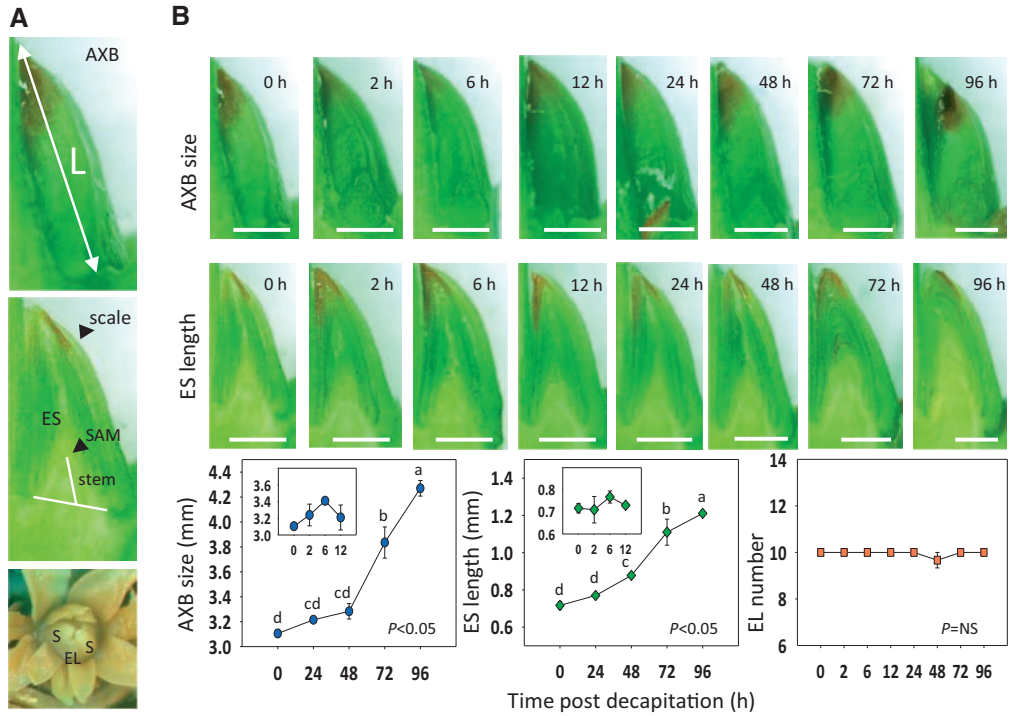

Fig. 4 AXB size, ES length and the number of embryonic leaves (EL) in the AXB proximal to the plant decapitation point. (A) The size of the AXBs was measured as indicated (L, upper panel). ES length was measured from the surface of the SAM to the basal line connecting the outer bud scales (middle panel). EL number, as depicted, was counted in fixed AXBs (lower panel). (B) Upper row photographs show AXB sizes, measured at 0, 2, 6, 12, 24, 48, 72 and 96 h post decapitation. The lower row shows ES lengths at the same time points. The line graphs show AXB size (left), ES length (middle) and EL number (right) at the indicated times after plant decapitation. Different letters indicate statistical differences between the time points (one-way ANOVA with *post hoc* Fisher's LSD test; *P*-value at least <0.05; NS, not significant). Scale bars, 1.0 mm.

GR24 (10 μM) was fed into the internode base of single-node systems for 3, 5 or 7 d. At day 3 (72 h), the young as well as the mature AXBs that were kept on water (controls) were already enlarging, while GR24-treated young and mature AXBs were slightly less elongated. However, at days 5 and 7 the effect was reversed, particularly in the case of mature AXBs (**Fig. 6**). The 7-d time point was repeated in a separate experiment, with a similar result. However, in both experiments, the promoting effect of GR24 on AXB size was not statistically significant (**Fig. 6**, inset). The sturdy outer scale of the mature AXBs did not elongate much, and AXB enlargement at day 7 was mostly due to the protrusion of the inner scales from the tip of the buds (Supplementary Fig. S4). GR24-feeding had a similar but more pronounced effect on the elongation of the ES. At the 7-d time point, the ESs of GR24-fed mature AXBs were significantly longer than the controls. The 7-d time point was repeated in a separate experiment, confirming that GR24 could enhance ES elongation once AXBs were activated (**Fig. 6**, inset).

Notably, in mature AXBs the number of embryonic leaves had increased from 10 to 12 by day 5 (120 h), and at day 7 (168 h) several additional primordia had emerged, with or without GR24. Young AXBs possessed fewer embryonic leaves at the time of single-node isolation, but also here the number rose steadily without any visible interruption. Although the GR24-fed young AXBs appeared to slightly delay leaf initiation, the differences in leaf numbers were not statistically significant (**Fig. 6**, inset).

Effects of GR24 on gene expression in AXBs of single-node systems

As GR24-feeding only affected the elongation of the ES in a statistically significant way, the early changes in gene expression must relate to ES elongation. Here, we investigated, how GR24-feeding would affect the SL pathway genes (**Fig. 1**) in mature and young AXBs. In the decapitation experiments, we probed the early changes in gene expression in the period preceding primordia formation (0–48 h). As in single-node systems, primordia formation started after day 3, we analyzed gene expression during an extended time-frame, including day 0, day 3 (72 h) and day 5 (120 h) (**Fig. 7**).

Whereas the *MAX1.1* and *MAX1.2* were highly expressed in young and mature AXBs (**Fig. 3C**), both genes were downregulated in AXBs in water, like in decapitation, except for *MAX1.2* in young AXBs. In all cases, GR24-feeding counteracted the change in expression (**Fig. 7A**), suggesting feedback on *MAX1* gene expression. Both, the downregulation and the counter-effect of GR24, were statistically significant for *MAX1.1*. In both young and mature AXBs, *D14a* and *D14b* were significantly upregulated without GR24, unlike in decapitation, while GR24-feeding repressed this completely (**Fig. 7B**). In young AXBs, *MAX2a* and *MAX2b* showed a similar response

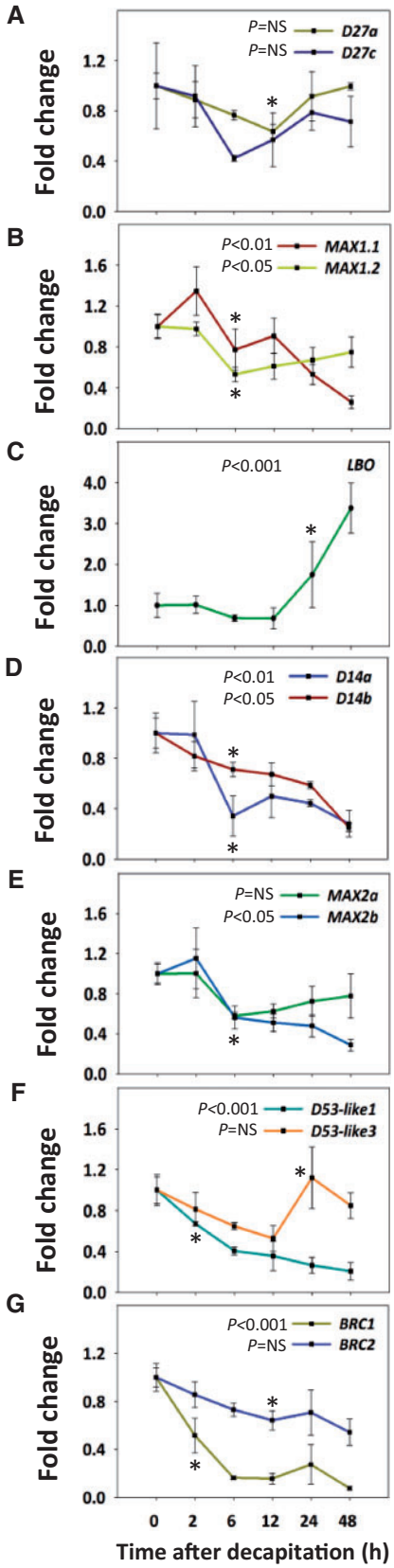

Fig. 5 Expression of SL pathway genes in AXBs proximal to the plant decapitation point. Gene expression (fold change) was analyzed at 0, 2, 6, 12, 24 and 48 h post decapitation. (A) *D27a* and *D27c*. (B) *MAX1.1* and *MAX1.2*. (C) *LBO*. (D) *D14a* and *D14b*. (E) *MAX2a* and *MAX2b*. (F) *D53-like1* and *D53-like3*. (G) *BRC1* and *BRC2*. Values represent the means of three biological replicates ±SE ($n = 6$ plants). Values were calculated relative to the AXBs at $t = 0$, set at 1. One-way ANOVA (*P*-value; NS, not significant). Asterisks indicate the first significant change in gene expression (Fisher's LSD test; *P*-value at least <0.05).

as the two *D14* genes in that both were significantly upregulated in water, while GR24 prevented this increase (Fig. 7C). Although in mature AXBs expression of *MAX2a* and *MAX2b* only slightly increased in the controls, GR24 had a statistically significant reducing effect on *MAX2a* (Fig. 7C).

D53-like1, encoding a putative repressor of SL signaling, was significantly downregulated in mature as well as in young AXBs, but GR24 prevented this decrease (Fig. 7D). This is in line with the decapitation experiments, where *D53-like1* was significantly downregulated already at day 1 and continued to decline up to 48 h (Fig. 5). Conversely, *D53-like3*, which is more closely related to *AtD53* than to *OsD53* (Supplementary Fig. S6), was upregulated in both young and mature AXBs in water, but GR24 prevented it in both cases (Fig. 7D). The increased expression of *D14a*, *D14b*, *MAX2a* and *MAX2b* in AXBs without GR24 could indicate that SL perception increased in response to diminished signal supply, reflecting homeostasis because GR24-feeding prevented upregulation of these genes. By contrast, the downstream target genes *BRC1* and *BRC2* were not significantly affected, except for *BRC1* in young AXBs.

In summary, the GR24-induced changes in expression of SL pathway genes in young and mature AXBs were quite similar, suggesting that the developmental stage is less important for the activation response. Although *MAX1.1*, *MAX1.2* and *D53-like1* were downregulated in the controls, *D14a*, *D14b*, *MAX2a*, *MAX2b* and *D53-like3* were upregulated. The only exception appeared to be *MAX1.2* in young AXBs, as it was not downregulated in controls. GR24-feeding counteracted these changes in all cases.

Discussion

The role of SL in shoot branching has been explored mainly in herbaceous plants (Gomez-Roldan et al. 2008, Umehara et al. 2008, Bennett and Leyser 2014, Marzec 2016, Waters et al. 2017, Barbier et al. 2019). This has yielded a wealth of data, showing that the studied species share the SL biosynthesis pathway that produces the universal precursor CLA, which is further converted to canonical and non-canonical SLs in a species-dependent fashion (Xie 2016, Iseki et al. 2018). The physiological relevance of this diversity has remained unclear (Zwanenburg and Blanco-Ania 2018). Although both canonical and non-canonical SLs are found in root exudates (Xie 2016, Iseki et al. 2018), tentative evidence shows that the SLs that regulate shoot branching are non-canonical (Yoneyama et al. 2018). How plants spatially and temporarily control the biosynthesis of the SLs that are involved in shoot branching has not been adequately addressed and remains an important research target (Kameoka and Kyozuka 2018).

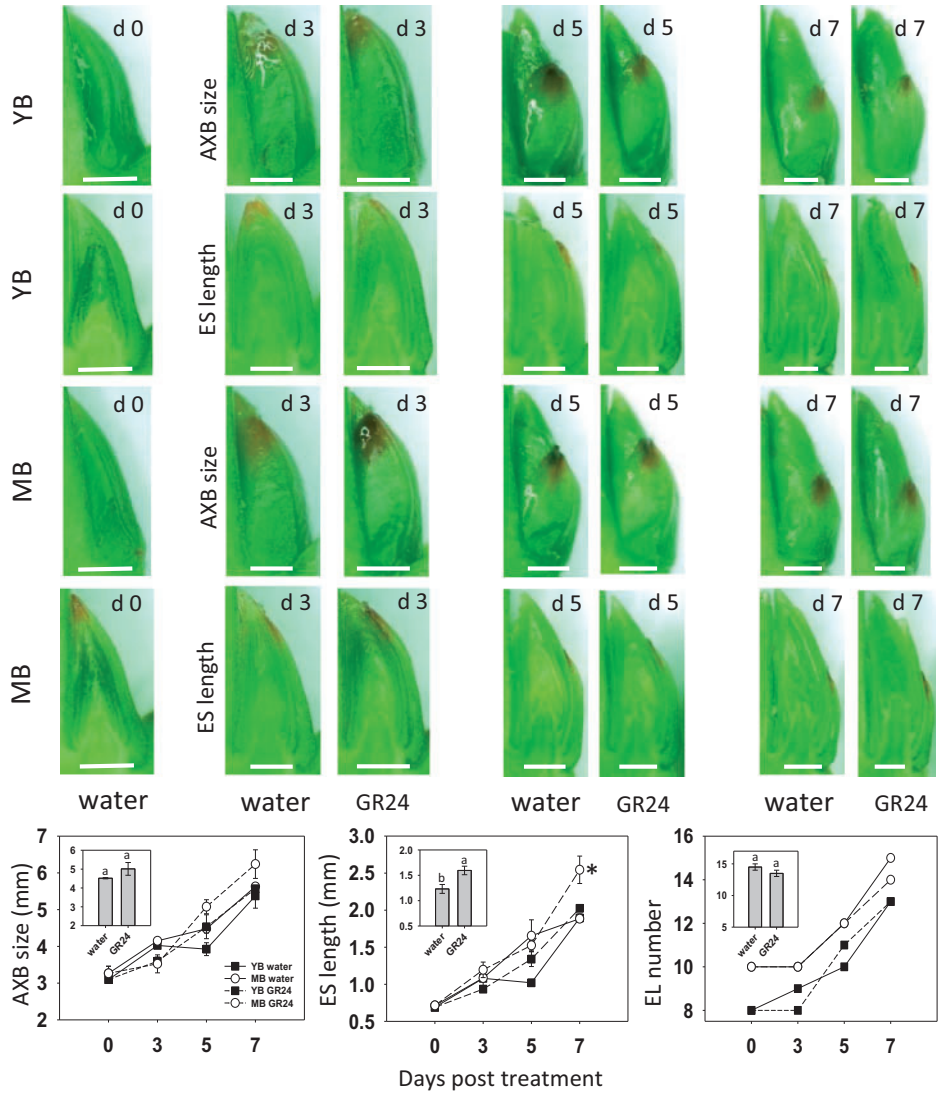

Fig. 6 AXB size, ES length and the number of embryonic leaves (EL) in young and mature AXBs (YB, MB) of single-node systems in water and GR24. Lengths of YB, MB and ES, as well as EL counts, were obtained as indicated in **Fig. 4A**. YBs and MBs: upper row photographs show example AXBs, and lower row photographs show longitudinally cut example AXBs at given days post isolation. The three line graphs show AXB size (left), ES length (middle) and EL number (right) at the indicated times after treatment with water and GR24. Insets: repeats of day 7. Different letters and asterisk indicate statistical differences (one-way ANOVA with post hoc Fischer's LSD test; *P*-value at least <0.05). Scale bars, 1.0 mm.

Especially, there is a need to better understand branching in trees, because their architecture, coupled to their superior CO_2 capture, is a critical element in mitigating climate change. To obtain more insight into the role of SLs in tree branching, we addressed the following questions. Are SL pathway and signaling genes conserved in the *Populus* genome? Is their expression spatially and functionally differentiated? Is the entire SL pathway operational in AXBs, independent of roots and shoot? Are SL biosynthesis and homeostasis affected by decapitation and GR24-feeding?

In addition to previously identified *Populus* homologs of SL biosynthesis and signaling genes (Czarnecki et al. 2014, Rinne et al. 2015, Muhr et al. 2016), we identified three homologs of *D27* (Supplementary Fig. S1), one of *LBO* (Supplementary Fig. S2) and three of *D53* (Supplementary Fig. S6). The existence of multiple copies in the *Populus* genome is a likely result of genome duplication (Tuskan et al. 2006). We found that the complete SL pathway of *Arabidopsis* and rice is conserved in *Populus* species and that in hybrid aspen the SL pathway genes show unique expression patterns (**Figs. 1**, **3**), which might relate to distinct features of tree branching. Firstly, the perennial lifestyle and the expansive shoot systems of trees (Tomlinson 1983, Millet et al. 1999, Barthélémy and Caraglio 2007, Ni et al. 2015, Rinne et al. 2015) require a modified branching strategy with a strong emphasis on mechanisms that act locally to control AXB outgrowth (**Fig. 8A**). Secondly, the AXBs, targets of SL signaling, are distinct in trees. In *Arabidopsis*, AXMs arise in axils of mature rosette leaves and produce simple scale-less buds (Grbić and Bleecker 2000, Long and Barton 2000). By contrast, in most trees, AXMs arise at a very early stage in the axils of emerging leaves and produce complex AXBs with an enclosed ES and sturdy bud scales (Garrison 1955, Paul et al. 2014, Rinne

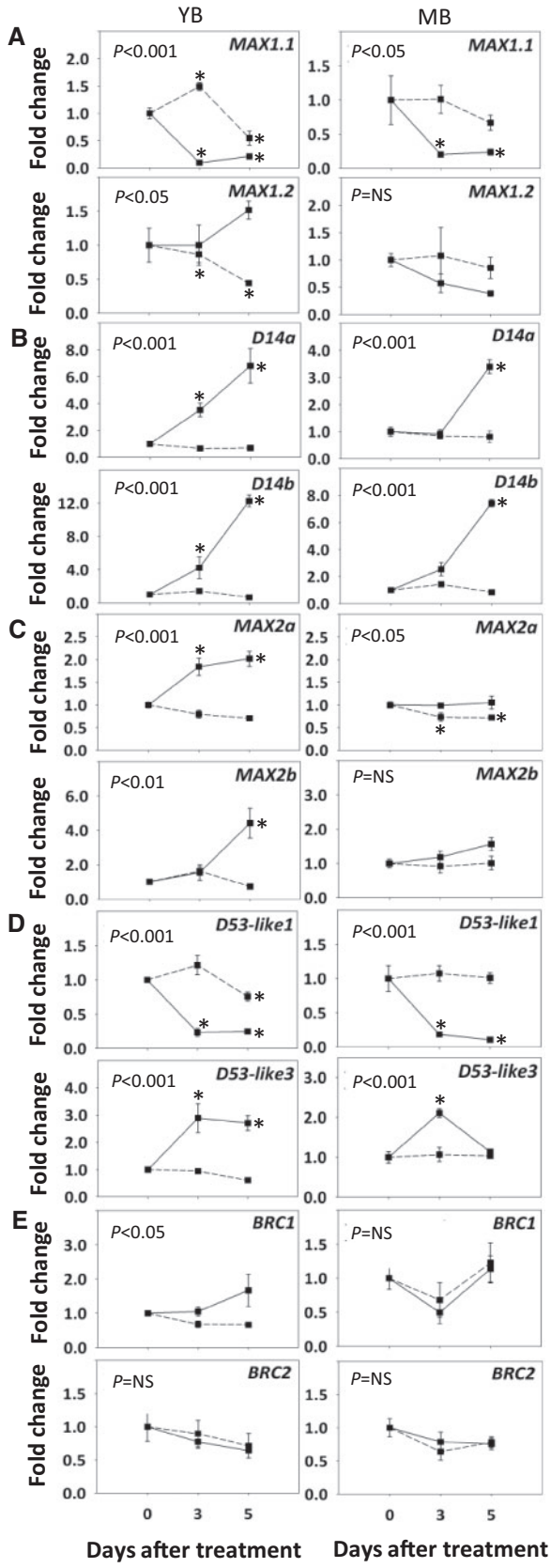

Fig. 7 Expression of SL pathway genes, downstream targets *BRC1* and *BRC2*, and the modulating effect of GR24. Young AXBs (YB, left column) and mature AXBs (MB, right column) on single-node systems in water control (–■–) and 10 μM GR24 (--■--). Gene expression was analyzed at 0, 3 and 5 d post isolation. (A) *MAX1.1* and *MAX1.2*. (B) *D14a* and *D14b*. (C) *MAX2a* and *MAX2b*. (D) *D53-like1* and *D53-like3*. (E) *BRC1* and *BRC2*. Values represent the means of three biological replicates ±SE ($n = 6$ plants). Values were calculated relative to the AXBs at $t = 0$, set at 1. Two-way ANOVA (*P*-value shows statistical significance between treatments; NS, not significant). Asterisks indicate significant differences with day 0 within each treatment (Fischer's LSD test; *P*-value at least <0.05).

et al. 2015). The outer scale presents a physical barrier that only gradually gives way (Supplementary Fig. S4).

Grafting experiments with herbaceous plants have shown that roots can act as the primary source for branch-inhibiting SLs (Beveridge et al. 2000, Morris et al. 2001, Turnbull et al. 2002, Simons et al. 2007). However, this does not necessarily reflect the situation in intact plants. Indeed, despite initial findings (Kohlen et al. 2011, Kohlen et al. 2012), xylem-transport of SL from roots to AXBs in intact plants has remained unconfirmed (Xie et al. 2015, Yoneyama et al. 2018). Nonetheless, our data indicate that AXBs in all likelihood receive CL and downstream products from elsewhere as, contrary to our initial assumption, AXBs themselves did not express *MAX3* and *MAX4*, but they did express the downstream biosynthetic gene *MAX1* (**Fig. 3B**). The few available studies on woody species did not detect *MAX3* and *MAX4* transcripts in AXBs and nodal bark, while *MAX4* was expressed only in wood tissue (Djennane et al. 2014, Muhr et al. 2016). Our data show that in hybrid aspen both genes are highly expressed in nodal bark tissues, and in addition in roots. Although root tips and bark tissues of source nodes expressed *MAX4* at similar levels, expression of *MAX3* was 65 times higher in the nodes. Moreover, in young nodes ('sink nodes'), *MAX3* and *MAX4* expressions were about 200 and 500 times higher, respectively, than in root tips (**Fig. 3B**). Based on our data, the bark of the AXB-associated nodes appears to be the main source of CL and downstream SL products. That in trees the nodes rather than the roots supply SLs to AXBs is a plausible conjecture, as it would allow for a more precise local control over branching of the expanding shoot system.

Young AXBs are active sinks that might import node-produced SLs along with sugars and other phloem-delivered compounds. As sugars can promote AXB outgrowth (Mason et al. 2014), a steady inflow of CL and SL-like compounds might be required to keep *BRC1* expression high in the maturing AXBs to prevent their outgrowth. Indeed, the expression of *MAX1* and *BRC1* steadily increases during AXB formation (Rinne et al. 2015). As *BRC1* and *BRC2* are class II TCPs, which repress cell cycling (Schommer et al. 2014), this suggests that during AXB formation SLs target *BRC1* to constrain the developing ES. Although the nodal bark expressed all SL biosynthesis genes, AXBs appeared to express *MAX1* and *LBO* (**Fig. 3C, D**), implying that they might convert imported CL and CLA, as well as MeCLA and other downstream products that require local conversion (**Figs. 1**, **8A**). That *LBO* is also expressed in the AXBs themselves is biologically meaningful, considering that its bioactive product, like MeCLA, is chemically unstable, providing

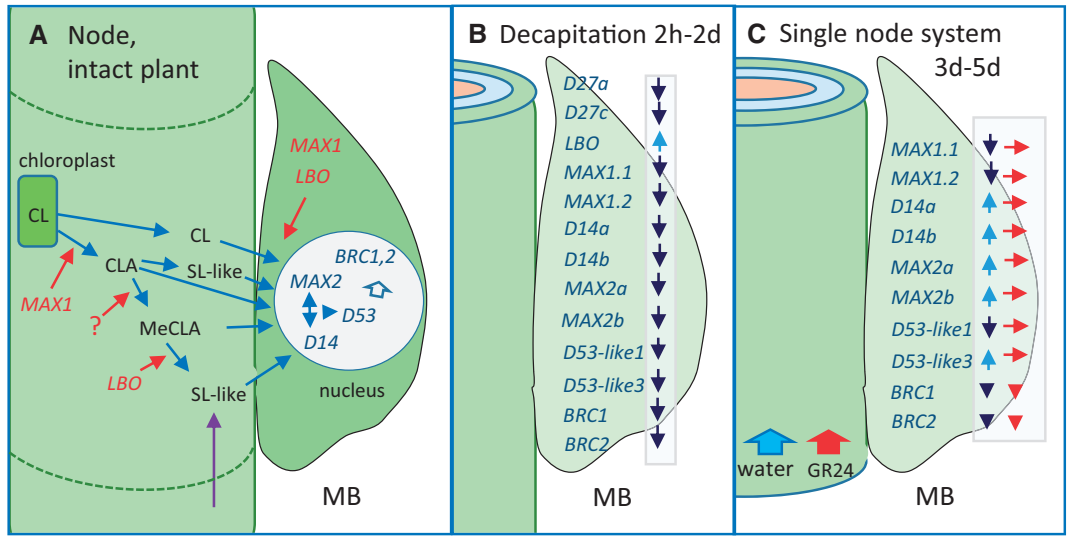

Fig. 8 Working models for mature AXBs (MBs) of proleptic hybrid aspen. (A) Node-to-bud signaling in intact plants. Nodes are dominant production centers of SLs, which are supplied to the AXBs. AXBs only express *MAX1* and *LBO*, which can convert imported CL, CLA, MeCLA (red arrow) into SL-like compounds that are hydrolyzed in nuclei by D14. Subsequent interaction with MAX2 results in ubiquitination and degradation of the transcription repressor D53. Downstream targets *BRC1* and *BRC2* inhibit AXB outgrowth. Roots hardly contribute SLs (purple arrow). Stippled lines delineate the node. (B) Proximal AXBs. All genes are initially downregulated (dark arrows) except for *LBO*, which is strongly upregulated (light blue arrow). (C) Single-node systems. *MAX1* genes are downregulated (dark arrows), but GR24-feeding (red arrow) prevents it through feedback (red arrows). *D14* and *MAX2* genes are upregulated (blue arrows), which is prevented by GR24-feeding (red arrows). *D53-like1* and *D53-like3* are, respectively, downregulated and upregulated (dark and blue arrows), but GR24-feeding prevents this (red arrows). *BRC1* and *BRC2* are modestly downregulated at day 3 (dark arrowheads), and GR24-feeding does not affect this (red arrowheads).

only weak inhibition of branching in a heterograft in *Arabidopsis* (Brewer et al. 2016).

Root tips also expressed *MAX3*, *MAX4*, *MAX1* as well as *LBO*, albeit at much lower levels than the nodes (**Fig. 3B–D**). Considering that e.g. *MAX2b* and *D53-like1* are hardly expressed in roots (**Fig. 3F, G**), root-produced SLs might serve specific root functions, including attraction of AM fungi in the rhizosphere. It is known that *Populus* roots can exude CLA, MeCLA as well as the canonical SL 4DO (Xie 2016). Although nodes of hybrid aspen expressed all SL pathway genes, including *D14* genes (**Fig. 3E**), *MAX2* genes (**Fig. 3F**) and *D53-like* genes (**Fig. 3G**), particularly *D14a* and *D14b* were expressed at much higher levels in the AXBs. The expression of *D14* in leaves (**Fig. 3E**) may take place in vascular tissues, as found for other species (Shen et al. 2007, Stirnberg et al. 2007, Zhou et al. 2013, Soundappan et al. 2015). As D14 is also present in the sieve tubes (Kameoka et al. 2016), by default it could move out of source leaves through mass flow toward sinks. Expression of SL pathway genes in vascular tissues may facilitate systemic bud–bud competition by modulation of auxin transport (Shinohara et al. 2013). Such systemic control by SL could also play a role in natural bud burst of hybrid aspen, for which AXBs require a pre-exposure to winter-chill that further upregulates the SL biosynthesis gene *MAX1* in AXBs (Rinne et al. 2018).

The role of LBO, which in *Arabidopsis* catalyzes the hydroxylation of MeCLA to the unidentified compound MeCLA+16D (Brewer et al. 2016), remains enigmatic in our study. Although expressed in all plant parts (**Fig. 3D**), its expression was highest in the nodes of the mature AXBs, which are poised for outgrowth, supporting its presumed role in inhibiting the outgrowth of para-dormant buds. Notably, expression of *LBO* in decapitation-activated AXBs was significantly increased after 1 d (**Fig. 5C**). As *BRC1* expression was already diminishing within 2 h, the increase in *LBO* expression might serve some as yet unidentified function. With the exception of *LBO*, the SL pathway genes were downregulated during the first 24 h in the bud activation process and followed by the start of ES elongation in the next 24 h (**Fig. 4B**).

The SL pathway has been shown to be subjected to homoeostatic control (Mashiguchi et al. 2009), like the GA pathway (Hedden and Thomas 2012). In single-node systems, the upregulation of receptor complex genes between days 3 and 5 could represent a response to diminished signal supply, considering the preceding downregulation of *MAX1* genes (**Fig. 7A**). Indeed, in support of this hypothesis, when signal supply was compensated by feeding GR24, the changes in the expression of the signaling genes were abolished (**Figs. 7B–D, 8C**). However, as most SL pathway genes may be subject to post-transcriptional and post-translational regulation (Zhou et al. 2013, Marzec and Muszynska 2015, Hu et al. 2017), this remains to be investigated.

It is unlikely that the initial triggers in decapitated plants and single-node systems are identical to those in natural branching because the constraints are different in all cases. For example, in decapitation experiments, the removal of the auxin-producing top part of the plant is crucial and could be the cause of AXB activation. However, in experiments with pea, auxin supply to the stump could not repress AXB outgrowth (Brewer et al. 2015). In hybrid aspen, the high expression of SL biosynthesis

genes in nodes of intact plants might prevent AXB activation in the intact plant, resulting in a proleptic branching style. Nonetheless, these high expression levels cannot prevent AXB outgrowth following decapitation. Sugar diversion (Mason et al. 2014, Kebrom 2017) might play a role also in decapitated hybrid aspen but is unlikely to be a factor in single-node systems that lack leaves. Although root-produced cytokinins (CK) are missing in this system, nodes might produce some CK as a result of the absence of a polar auxin transport stream (Nordström et al. 2004, Tanaka et al. 2006, Ferguson and Beveridge 2009).

Our data show that GR24-feeding cannot prevent outgrowth once AXBs are activated. As CK as well as GA can be locally produced in nodes and AXBs, it seems possible that they synergistically promote AXB activation, overriding SL effects by repressing *MAX2* and the downstream effects on *BRC1* (Ni et al. 2015). Indeed, we showed that decapitation upregulates GA biosynthesis genes in AXBs (Rinne et al. 2016), whereas SL pathway genes are downregulated (Fig. 5). GA not only represses SL perception, but it can also downregulate SL biosynthesis (Ni et al. 2015, Ito et al. 2017, Marzec 2017). Moreover, GA also reinvigorates symplasmic stem–bud connections by upregulating 1,3-β-glucanase genes (Rinne et al. 2011, Rinne et al. 2016), thereby potentially facilitating import of sugars and other nutrients to drive AXB outgrowth.

Conclusions

Nodes rather than distant roots may supply SL precursors and SLs to AXBs, whereas AXBs are sites of SL perception and *BRC1* action (Fig. 8). Mature AXBs can also synthesize SL-like compounds downstream of CL, but probably not CL itself as *MAX3* and *MAX4* are not expressed in AXBs, while *MAX1* and *LBO* are (Figs. 3B–D, 8A). As most SL pathway genes are downregulated by decapitation within hours, and ahead of ES elongation, SL might function in intact plants to inhibit AXB activation. Once activated, elongation of the ES might even be promoted by SL, as suggested by GR24-feeding of single-node systems. GR24-feeding data also support the notion that SL pathway genes are under homeostatic control. When apically produced auxin, root-produced cytokinins and leaf produced sugars are lacking, AXB still grow out despite high initial levels of SL gene expression in nodes, even after GR24-feeding. Although the initial triggers of AXB activation differ between intact plants, decapitated plants and single-node systems, the ensuing growth processes rapidly converge. SLs may restrain outgrowth only during AXB formation and para-dormancy in intact plants but cannot override the interacting factors that facilitate outgrowth of activated AXBs.

Materials and Methods

Plant material and sampling

Hybrid aspen (*P. tremula* × *P. tremuloides*) clone T89 was micro-propagated in vitro for 5 weeks in 20°C, planted in a mixture of soil/peat and perlite [4:1 (v/v)], fertilized with 4 $g \cdot l^{-1}$ Osmocote, grown in a greenhouse under long days (18 h light) at 20°C and 60% relative humidity, and watered twice a day. Natural daylight was supplemented by mercury-halide lamps with the lighting of 200–250 $\mu mol \cdot m^{-2} \cdot s^{-1}$ (Osram) to maintain an 18 h photoperiod. The plants were replanted in 13 cm pots when they were ca. 60 cm high. Experiments were started when the plants had reached a height of 80–100 cm, and leaf production rates and elongation were stable. The plants were subdivided into three groups. Group one was kept in long-day (LD) conditions and decapitated at the BMP (Fig. 2), at around 40 cm below the apex, to eliminate apical dominance. The position of the BMP was as described by Rinne et al. (2015). Group two was kept in LD to collect various types of tissues and organs from intact plants. Group three plants were used for xylem-feeding experiments with single-node systems.

Measurements of AXB and embryonic shoot length, and embryonic leaf number

To record the developmental changes in AXBs proximal to the decapitation point AXB length was measured at 0, 2, 6, 12, 24, 48, 72 and 96 h post decapitation. At the same time points, the AXBs were cut longitudinally under a dissection microscope, and the length of the enclosed ES was measured from the top of the SAM to the middle of a line connecting the base of the outer scale (Fig. 4A). Lastly, comparable AXBs were fixed in 70% alcohol for assessing the neo-formation of leaves. Under a dissection microscope, the bud scales were peeled away, and the number of embryonic leaves was counted for each time point. Commonly the SAM contained one leaf buttress, which was included in the count.

AXB burst tests and GR24-feeding

To investigate the role of SL in AXB inhibition, we performed xylem-feeding experiments in combination with AXB burst tests under forcing conditions. As hybrid aspen is proleptic, the forced activation of AXBs represents a form of bud burst which, in contrast to sylleptic species and herbaceous plants, includes two processes, activation and outgrowth. For xylem-feeding, single-node systems without leaves were isolated from 6-week-old LD plants. The internode base was punched through pores in a Styrofoam sheet that was floated on water (control) or water supplemented with the synthetic SL analog (rac-GR24; Chiralix BV, The Netherlands) at a concentration of 10 μM. In preliminary experiment GR24 in concentrations of 1, 5 and 10 μM were tested, and 10 μM was chosen for the current experiments. In each treatment and time point, three replicates of young and three replicates of mature AXBs were used. AXB length, ES length and embryonic leaf number were recorded at days 0, 3, 5 and 7. The young buds and the mature AXBs below the BMP were harvested at days 0, 3 and 5 to analyze changes in the relative expression of SL pathway genes induced by decapitation, and by the combination of decapitation and GR24-feeding. The experiments were repeated at least twice.

Gene selection and identification

To examine the expression patterns of SL biosynthesis and signaling genes in 6-week-old intact plants, total RNA was extracted from different plant parts. These included the apex, young AXBs, the bark of the corresponding node of young AXBs ('sink node'), sink leaves, mature para-dormant AXBs, the corresponding node of mature AXBs ('source node'), source leaves and root tips (Fig. 2). In total, three AXBs above, and three below the BMP, as well as other tissues like indicated above, were collected from each of the six plants. Samples of two plants were pooled to obtain three biological replicates. Gene expression analyzes included *Populus* homologs of the *Arabidopsis* SL biosynthesis and signaling genes *D27a*, *D27b*, *D27c*, *MAX1.1*, *MAX1.2*, *LBO*, *MAX3*, *MAX4*, *D14a*, *D14b*, *MAX2a*, *MAX2b*, *D53-like1*, *D53-like2*, *D53-like3*, as well as the downstream target genes *BRC1* and *BRC2*.

To assess decapitation-induced changes in gene expression, mature AXBs proximal to the decapitation point at the BMP (Fig. 2) were collected at days 0, 2, 6, 12, 24 and 48 h post decapitation. For each time point, RNA was extracted from three biological replicates, pooled as described above. Sampling after day 1 (24 h) and day 2 (48 h) were carried out at the same time of the day to avoid potential diurnal effects on gene expression.

To assess the role of exogenous SL on gene expression in AXBs of single-node systems, they were incubated in water with or without GR24. AXBs were collected after 0, 3 and 5 d of treatment. Gene expression was assessed for the SL biosynthesis genes *D27a*, *D27c*, *MAX1.1* and *MAX1.2*, as well as the SL signaling genes *D14a*, *D14b*, *MAX2a*, *MAX2b*, *D53-like1*, *D53-like2*, *D53-like3* and downstream targets *BRC1* and *BRC2*.

RNA extraction, cDNA preparation and quantitative RT-PCR analysis

Total RNA was extracted from 0.2 to 0.3 g of frozen tissue and grinded in a mortar with 500 µl extraction buffer (Qiagen RLT buffer containing 1% PVP-40), followed by an addition of a 0.4 volume KoAC (pH 6.5) and further homogenization. Subsequently, the solution was transferred to a 2-ml tube, incubated on ice for 15 min, and centrifuged at 12,000 rpm at 4°C for 15 min. The supernatant was transferred to a new 1.5-ml tube, and a 0.5 ml volume of 100% ethanol was added. The mix was transferred to RNeasy spin columns and further processed in accordance with instructions of the Qiagen Plant RNA isolation kit. Genomic DNA was eliminated using TURBO™ DNase kit (Invitrogen) treatment according to the manufacturer's instructions and cleaned using the total RNA purification system 'Purelink RNA mini kit' (Invitrogen). RNA was quantified with NanoDrop 1000, and the RNA quality was assessed with the Agilent 2100 Bioanalyzer system. One microgram of total RNA was reversely transcribed to cDNA with SuperScript® VILO™ reverse transcriptase (Invitrogen). Quantitative RT-PCR (qRT-PCR) was used to analyze transcript levels of all SL pathway genes. The reaction setup (20 µl total volume) was prepared using SYBR® select PCR master mix (Applied Biosystems). As a template, 2 µl of the cDNA (200 ng) were added. All the qPCR reactions were run with three biological replicates and analyzed in three technical repeats. Real-time qRT-PCR analyses were performed with the Applied Biosystems 7500 Fast Real-Time PCR system according to the manufacturer's instruction. Thermocycling conditions were set to 50°C for 2 min, 95°C for 2 min, 45 cycles of 15 s at 95°C and 60 s at 60°C. In addition, each PCR reaction included a negative control to check for potential genomic DNA contamination. PCR amplification of *Populus actin* served as a reference gene for normalizing the relative transcript level. For a complete list of primers and genes used for qRT-PCR see Supplementary Table S1.

Statistical analysis

Statistical analyses were carried out using analysis of variance (ANOVA) in combination with a post hoc test to determine significant differences between the subgroups. One-way ANOVA in combination with Fisher's LSD test was computed to monitor the decapitation-induced changes in transcript levels and to pinpoint the time within the 48 h trajectory when a significant change took place. To analyze the effect of GR24 on gene expression during the 7-d feeding experiment, two-way ANOVA (time and treatment as factors) was used in combination with Fisher's LSD multiple comparison test. The developmental changes during AXB activation (AXB length, ES elongation, leaf numbers) induced either by decapitation or isolation of the single-node systems and treated with or without GR24 were analyzed with one- or two-way ANOVA and combined with Fisher's LSD test. Computation was performed using Microsoft Excel data analysis (www.microsoft.com) and Minitab Statistical Software version 18.1 (www.minitab.com).

Bioinformatics

BLAST searches in GenBank, *P. trichocarpa* genome v3.0 and *P. tremula* × *P. tremuloides* (T89) v0.1 databases (http://www.ncbi.nlm.nih.gov/BLAST; http://www.phytozome.net; http://popgenie.org/) were used to identify SL biosynthesis and signaling genes. Gene-specific primer sequences for qPCR analysis were designed using Primer3 (http://bioinfo.ut.ee/primer3-0.4.0/). Phylogenetic trees were created using the MEGA6 program (www.megasoftware.net) with the Neighbor–Joining method. Bootstrap support values are based on 1,000 replicates.

Supplementary Data

Supplementary data are available at PCP online.

Funding

The Norwegian University of Life Sciences to NUK, and a FRIPRO grant of the Norwegian Research Council to CvdS and PLHR [nr. 263117].

Acknowledgments

We acknowledge the financial support of the Norwegian University of Life Sciences and the Norwegian Research Council. We thank Marit Siira for excellent help with the plants, and Manikandan Veerabagu for helpful discussions. We are grateful for the thoughtful and constructive comments of the anonymous reviewers.

Disclosures

The authors have no conflicts of interest to declare.

References

Abe, S., Sado, A., Tanaka, K., Kisugi, T., Asami, K., Ota, S., et al. (2014) Carlactone is converted to carlactonoic acid by MAX1 in *Arabidopsis* and its methyl ester can directly interact with AtD14 in vitro. *Proc. Natl. Acad. Sci. USA* 111: 18084–18089.

Aguilar-Martínez, J.A., Poza-Carrión, C. and Cubas, P. (2007) *Arabidopsis BRANCHED1* acts as an integrator of branching signals within axillary buds. *Plant Cell* 19: 458–472.

Akiyama, K., Matsuzaki, K-I. and Hayashi, H. (2005) Plant sesquiterpenes induce hyphal branching in arbuscular mycorrhizal fungi. *Nature* 435: 824–827.

Alder, A., Jamil, M., Marzorati, M., Bruno, M., Vermathen, M., Bigler, P., et al. (2012) The path from β-carotene to carlactone, a strigolactone-like plant hormone. *Science* 335: 1348–1351.

Barbier, F.F., Dun, E.A., Kerr, S.C., Chabikwa, T.G. and Beveridge, C.A. (2019) An update on the signals controlling shoot branching. *Trends Plant Sci.* 24: 220–236.

Barthélémy, D. and Caraglio, Y. (2007) Plant architecture: a dynamic, multilevel and comprehensive approach to plant form, structure and ontogeny. *Ann. Bot.* 99: 375–407.

Bennett, T. and Leyser, O. (2014) Strigolactone signalling: standing on the shoulders of DWARFs. *Curr. Opin. Plant Biol.* 22: 7–13.

Besserer, A., Puech-Pagès, V., Kiefer, P., Gomez-Roldan, V., Jauneau, A., Roy, S., et al. (2006) Strigolactones stimulate arbuscular mycorrhizal fungi by activating mitochondria. *PLoS Biol.* 4: e226.

Beveridge, C.A., Symons, G.M., Murfet, I.C., Ross, J.J. and Rameau, C. (1997) The *rms1* mutant of pea has elevated indole-3-acetic acid levels and reduced root-sap zeatin riboside content but increased branching controlled by graft-transmissible signal(s). *Plant Physiol.* 115: 1251–1258.

Beveridge, C.A., Symons, G.M. and Turnbull, C.G. (2000) Auxin inhibition of decapitation-induced branching is dependent on graft-transmissible signals regulated by genes *Rms1* and *Rms2*. *Plant Physiol.* 123: 689–698.

Booker, J., Auldridge, M., Wills, S., McCarty, D., Klee, H. and Leyser, O. (2004) MAX3/CCD7 is a carotenoid cleavage dioxygenase required for the synthesis of a novel plant signaling molecule. *Curr. Biol.* 14: 1232–1238.

Booker, J., Sieberer, T., Wright, W., Williamson, L., Willett, B., Stirnberg, P., et al. (2005) *MAX1* encodes a cytochrome P450 family member that acts downstream of *MAX3/4* to produce a carotenoid-derived branch-inhibiting hormone. *Dev. Cell* 8: 443–449.

Brewer, P.B., Dun, E.A., Gui, R., Mason, M.G. and Beveridge, C.A. (2015) Strigolactone inhibition of branching independent of polar auxin transport. *Plant Physiol.* 168: 1820–1829.

Brewer, P.B., Yoneyama, K., Filardo, F., Meyers, E., Scaffidi, A., Frickey, T., et al. (2016) *LATERAL BRANCHING OXIDOREDUCTASE* acts in the final stages of strigolactone biosynthesis in *Arabidopsis*. *Proc. Natl. Acad. Sci. USA* 113: 6301–6306.

Carbonnel, S. and Gutjahr, C. (2014) Control of arbuscular mycorrhiza development by nutrient signals. *Front. Plant Sci.* 5: 462.

Ceulemans, R., Stettler, R., Hinckley, T., Isebrands, J. and Heilman, P. (1990) Crown architecture of *Populus* clones as determined by branch orientation and branch characteristics. *Tree Physiol.* 7: 157–167.

Chevalier, F., Nieminen, K., Sánchez-Ferrero, J.C., Rodríguez, M.L., Chagoyen, M., Hardtke, C.S., et al. (2014) Strigolactone promotes degradation of DWARF14, an α/β hydrolase essential for strigolactone signaling in *Arabidopsis*. *Plant Cell* 26: 1134–1150.

Cline, M.G. (1997) Concepts and terminology of apical dominance. *Am. J. Bot.* 84: 1064–1069.

Cook, C., Whichard, L.P., Turner, B., Wall, M.E. and Egley, G.H. (1966) Germination of witchweed (*Striga lutea* Lour.): isolation and properties of a potent stimulant. *Science* 154: 1189–1190.

Cook, C., Whichard, L.P., Wall, M., Egley, G.H., Coggon, P., Luhan, P.A., et al. (1972) Germination stimulants. II. Structure of strigol, a potent seed germination stimulant for witchweed (*Striga lutea* Lour.). *J. Am. Chem. Soc.* 94: 6198–6199.

Czarnecki, O., Yang, J., Wang, X., Wang, S., Muchero, W., Tuskan, G.A., et al. (2014) Characterization of *MORE AXILLARY GROWTH* genes in *Populus*. *PLoS One* 9: e102757.

Djennane, S., Hibrand-Saint Oyant, L., Kawamura, K., Lalanne, D., Laffaire, M., Thouroude, T., et al. (2014) Impacts of light and temperature on shoot branching gradient and expression of strigolactone synthesis and signalling genes in rose. *Plant Cell Environ.* 37: 742–757.

Doebley, J., Stec, A. and Hubbard, L. (1997) The evolution of apical dominance in maize. *Nature* 386: 485–488.

Domagalska, M.A. and Leyser, O. (2011) Signal integration in the control of shoot branching. *Nat. Rev. Mol. Cell Biol.* 12: 211–221.

Drummond, R.S., Martínez-Sánchez, N.M., Janssen, B.J., Templeton, K.R., Simons, J.L., Quinn, B.D., et al. (2009) *Petunia hybrida CAROTENOID CLEAVAGE DIOXYGENASE7* is involved in the production of negative and positive branching signals in petunia. *Plant Physiol.* 151: 1867–1877.

Ferguson, B.J. and Beveridge, C.A. (2009) Roles for auxin, cytokinin, and strigolactone in regulating shoot branching. *Plant Physiol.* 149: 1929–1944.

Finlayson, S.A. (2007) *Arabidopsis* TEOSINTE BRANCHED1-LIKE1 regulates axillary bud outgrowth and is homologous to monocot TEOSINTE BRANCHED1. *Plant Cell Physiol.* 48: 667–677.

Finlayson, S.A., Krishnareddy, S.R., Kebrom, T.H. and Casal, J.J. (2010) Phytochrome regulation of branching in *Arabidopsis*. *Plant Physiol.* 152: 1914–1927.

Garrison, R. (1955) Studies in the development of axillary buds. *Am. J. Bot.* 42: 257–266.

Gomez-Roldan, V., Fermas, S., Brewer, P.B., Puech-Pagès, V., Dun, E.A., Pillot, J.-P., et al. (2008) Strigolactone inhibition of shoot branching. *Nature* 455: 189–194.

Grbić, V. and Bleecker, A.B. (2000) Axillary meristem development in *Arabidopsis thaliana*. *Plant J.* 21: 215–223.

Greb, T., Clarenz, O., Schäfer, E., Müller, D., Herrero, R., Schmitz, G., et al. (2003) Molecular analysis of the *LATERAL SUPPRESSOR* gene in *Arabidopsis* reveals a conserved control mechanism for axillary meristem formation. *Genes Dev.* 17: 1175–1187.

Hallé, F., Oldeman, R.A. and Tomlinson, P.B. (1978) Tropical Trees and Forests. An Architectural Analysis. p. 444. Springer, Berlin; Heidelberg; New York.

Hamiaux, C., Drummond, R.S., Janssen, B.J., Ledger, S.E., Cooney, J.M., Newcomb, R.D., et al. (2012) DAD2 is an α/β hydrolase likely to be involved in the perception of the plant branching hormone, strigolactone. *Curr. Biol.* 22: 2032–2036.

Hedden, P. and Thomas, S.G. (2012) Gibberellin biosynthesis and its regulation. *Biochem. J.* 444: 11–25.

Hu, Q., He, Y., Wang, L., Liu, S., Meng, X., Liu, G., et al. (2017) DWARF14, a receptor covalently linked with the active form of strigolactones, undergoes strigolactone-dependent degradation in rice. *Front. Plant Sci.* 8: 1935.

Iseki, M., Shida, K., Kuwabara, K., Wakabayashi, T., Mizutani, M., Takikawa, H., et al. (2018) Evidence for species-dependent biosynthetic pathways for converting carlactone to strigolactones in plants. *J. Exp. Bot.* 69: 2305–2318.

Ito, S., Yamagami, D., Umehara, M., Hanada, A., Yoshida, S., Sasaki, Y., et al. (2017) Regulation of strigolactone biosynthesis by gibberellin signaling. *Plant Physiol.* 174: 1250–1259.

Jiang, L., Liu, X., Xiong, G., Liu, H., Chen, F., Wang, L., et al. (2013) DWARF 53 acts as a repressor of strigolactone signalling in rice. *Nature* 504: 401–405.

Kameoka, H., Dun, E.A., Lopez-Obando, M., Brewer, P.B., de Saint Germain, A., Rameau, C., et al. (2016) Phloem transport of the receptor DWARF14 protein is required for full function of strigolactones. *Plant Physiol.* 172: 1844–1852.

Kameoka, H. and Kyozuka, J. (2018) Spatial regulation of strigolactone function. *J. Exp. Bot.* 69: 2255–2264.

Kapulnik, Y., Delaux, P.-M., Resnick, N., Mayzlish-Gati, E., Wininger, S., Bhattacharya, C., et al. (2011) Strigolactones affect lateral root formation and root-hair elongation in *Arabidopsis*. *Planta* 233: 209–216.

Kebrom, T.H. (2017) A growing stem inhibits bud outgrowth–the overlooked theory of apical dominance. *Front. Plant Sci.* 8: 1874.

King, R. and Van Staden, J. (1988) Differential responses of buds along the shoot of *Pisum sativum* to isopentenyladenine and zeatin application. *Plant Physiol. Biochem.* 20: 253–259.

Kobae, Y., Kameoka, H., Sugimura, Y., Saito, K., Ohtomo, R., Fujiwara, T., et al. (2018) Strigolactone biosynthesis genes of rice are required for the punctual entry of arbuscular mycorrhizal fungi into the roots. *Plant Cell Physiol.* 59: 544–553.

Kohlen, W., Charnikhova, T., Lammers, M., Pollina, T., Tóth, P., Haider, I., et al. (2012) The tomato *CAROTENOID CLEAVAGE DIOXYGENASE 8* (*SlCCD8*) regulates rhizosphere signaling, plant architecture and affects reproductive development through strigolactone biosynthesis. *New Phytol.* 196: 535–547.

Kohlen, W., Charnikhova, T., Liu, Q., Bours, R., Domagalska, M.A., Beguerie, S., et al. (2011) Strigolactones are transported through the xylem and play a key role in shoot architectural response to phosphate deficiency in nonarbuscular mycorrhizal host *Arabidopsis*. *Plant Physiol.* 155: 974–987.

Liang, Y., Ward, S., Li, P., Bennett, T. and Leyser, O. (2016) SMAX1-LIKE7 signals from the nucleus to regulate shoot development in *Arabidopsis* via partially EAR motif-independent mechanisms. *Int. J. Mol. Sci.* 28: 1581–1601.

Lin, H., Wang, R., Qian, Q., Yan, M., Meng, X., Fu, Z., et al. (2009) DWARF27, an iron-containing protein required for the biosynthesis of strigolactones, regulates rice tiller bud outgrowth. *Plant Cell* 21: 1512–1525.

Long, J. and Barton, M.K. (2000) Initiation of axillary and floral meristems in *Arabidopsis*. *Dev. Biol.* 218: 341–353.

López-Ráez, J.A., Charnikhova, T., Gómez-Roldán, V., Matusova, R., Kohlen, W., De Vos, R., et al. (2008) Tomato strigolactones are derived from carotenoids and their biosynthesis is promoted by phosphate starvation. *New Phytol.* 178: 863–874.

Marzec, M. (2016) Perception and signaling of strigolactones. *Front. Plant Sci.* 7: 1260.

Marzec, M. (2017) Strigolactones and gibberellins: a new couple in the phytohormone world? *Trends Plant Sci.* 22: 813–815.

Marzec, M. and Muszynska, A. (2015) *In silico* analysis of the genes encoding proteins that are involved in the biosynthesis of the RMS/MAX/D

pathway revealed new roles of strigolactones in plants. *Int. J. Mol. Sci.* 16: 6757–6782.

Mashiguchi, K., Sasaki, E., Shimada, Y., Nagae, M., Ueno, K., Nakano, T., et al. (2009) Feedback-regulation of strigolactone biosynthetic genes and strigolactone-regulated genes in *Arabidopsis*. *Biosci. Biotechnol. Biochem*. 73: 2460–2465.

Mason, M.G., Ross, J.J., Babst, B.A., Wienclaw, B.N. and Beveridge, C.A. (2014) Sugar demand, not auxin, is the initial regulator of apical dominance. *Proc. Natl. Acad. Sci. USA* 111: 6092–6097.

Matusova, R., Rani, K., Verstappen, F.W., Franssen, M.C., Beale, M.H. and Bouwmeester, H.J. (2005) The strigolactone germination stimulants of the plant-parasitic *Striga* and *Orobanche* spp. are derived from the carotenoid pathway. *Plant Physiol.* 139: 920–934.

Millet, J., Bouchard, A. and Édelin, C. (1999) Relationship between architecture and successional status of trees in the temperate deciduous forest. *Écoscience* 6: 187–203.

Morris, S.E., Turnbull, C.G., Murfet, I.C. and Beveridge, C.A. (2001) Mutational analysis of branching in pea. Evidence that *Rms1* and *Rms5* regulate the same novel signal. *Plant Physiol.* 126: 1205–1213.

Muhr, M., Paulat, M., Awwanah, M., Brinkkötter, M. and Teichmann, T. (2018) CRISPR/Cas9-mediated knockout of *Populus BRANCHED1* and *BRANCHED2* orthologs reveals a major function in bud outgrowth control. *Tree Physiol*. 38: 1588–1597.

Muhr, M., Prüfer, N., Paulat, M. and Teichmann, T. (2016) Knockdown of strigolactone biosynthesis genes in *Populus* affects *BRANCHED1* expression and shoot architecture. *New Phytol.* 212: 613–626.

Müller, D. and Leyser, O. (2011) Auxin, cytokinin and the control of shoot branching. *Ann. Bot.* 107: 1203–1212.

Ni, J., Gao, C., Chen, M.-S., Pan, B.-Z., Ye, K. and Xu, Z.-F. (2015) Gibberellin promotes shoot branching in the perennial woody plant *Jatropha curcas*. *Plant Cell Physiol.* 56: 1655–1666.

Nordström, A., Tarkowski, P., Tarkowska, D., Norbaek, R., Åstot, C., Dolezal, K., et al. (2004) Auxin regulation of cytokinin biosynthesis in *Arabidopsis thaliana*: a factor of potential importance for auxin–cytokinin-regulated development. *Proc. Natl. Acad. Sci. USA* 101: 8039–8044.

Paul, L.K., Rinne, P.L. and van der Schoot, C. (2014) Shoot meristems of deciduous woody perennials: self-organization and morphogenetic transitions. *Curr. Opin. Plant Biol*. 17: 86–95.

Rasmussen, A., Mason, M.G., De Cuyper, C., Brewer, P.B., Herold, S., Agusti, J., et al. (2012) Strigolactones suppress adventitious rooting in *Arabidopsis* and pea. *Plant Physiol.* 158: 1976–1987.

Rinne, P.L., Paul, L.K., Vahala, J., Kangasjärvi, J. and van der Schoot, C. (2016) Axillary buds are dwarfed shoots that tightly regulate GA pathway and GA-inducible 1, 3-β-glucanase genes during branching in hybrid aspen. *J. Exp. Bot.* 67: 5975–5991.

Rinne, P.L., Paul, L.K., Vahala, J., Ruonala, R., Kangasjärvi, J. and van der Schoot, C. (2015) Long and short photoperiod buds in hybrid aspen share structural development and expression patterns of marker genes. *J. Exp. Bot.* 66: 6745–6760.

Rinne, P.L., Paul, L.K. and van der Schoot, C. (2018) Decoupling photo-and thermoperiod by projected climate change perturbs bud development, dormancy establishment and vernalization in the model tree *Populus*. *BMC Plant Biol.* 18: 220.

Rinne, P.L., Welling, A., Vahala, J., Ripel, L., Ruonala, R., Kangasjärvi, J., et al. (2011) Chilling of dormant buds hyperinduces *FLOWERING LOCUS T* and recruits GA-inducible 1, 3-β-glucanases to reopen signal conduits and release dormancy in *Populus*. *Plant Cell* 23: 130–146.

Scaffidi, A., Waters, M.T., Ghisalberti, E.L., Dixon, K.W., Flematti, G.R. and Smith, S.M. (2013) Carlactone-independent seedling morphogenesis in *Arabidopsis*. *Plant J.* 76: 1–9.

Schommer, C., Debernardi, J.M., Bresso, E.G., Rodriguez, R.E. and Palatnik, J.F. (2014) Repression of cell proliferation by miR319-regulated TCP4. *Mol. Plant.* 7: 1533–1544.

Seale, M., Bennett, T. and Leyser, O. (2017) *BRC1* expression regulates bud activation potential, but is not necessary or sufficient for bud growth inhibition in *Arabidopsis*. *Development* 144: 1661–1673.

Seto, Y. and Yamaguchi, S. (2014) Strigolactone biosynthesis and perception. *Curr. Opin. Plant Biol*. 21: 1–6.

Shen, H., Luong, P. and Huq, E. (2007) The F-box protein MAX2 functions as a positive regulator of photomorphogenesis in *Arabidopsis*. *Plant Physiol.* 145: 1471–1483.

Shinohara, N., Taylor, C. and Leyser, O. (2013) Strigolactone can promote or inhibit shoot branching by triggering rapid depletion of the auxin efflux protein PIN1 from the plasma membrane. *PLoS Biol.* 11: e1001474.

Simons, J.L., Napoli, C.A., Janssen, B.J., Plummer, K.M. and Snowden, K.C. (2007) Analysis of the *DECREASED APICAL DOMINANCE* genes of petunia in the control of axillary branching. *Plant Physiol.* 143: 697–706.

Sorefan, K., Booker, J., Haurogné, K., Goussot, M., Bainbridge, K., Foo, E., et al. (2003) *MAX4* and *RMS1* are orthologous dioxygenase-like genes that regulate shoot branching in *Arabidopsis* and pea. *Genes Dev*. 17: 1469–1474.

Soundappan, I., Bennett, T., Morffy, N., Liang, Y., Stanga, J.P., Abbas, A., et al. (2015) SMAX1-LIKE/D53 family members enable distinct MAX2-dependent responses to strigolactones and karrikins in *Arabidopsis*. *Plant Cell* 27: 3143–3159.

Stirnberg, P., Furner, I.J. and Ottoline Leyser, H. (2007) MAX2 participates in an SCF complex which acts locally at the node to suppress shoot branching. *Plant J.* 50: 80–94.

Tanaka, M., Takei, K., Kojima, M., Sakakibara, H. and Mori, H. (2006) Auxin controls local cytokinin biosynthesis in the nodal stem in apical dominance. *Plant J.* 45: 1028–1036.

Tomlinson, P. (1983) Tree architecture: new approaches help to define the elusive biological property of tree form. *Am. Sci*. 71: 141–149.

Turnbull, C.G., Booker, J.P. and Leyser, H.O. (2002) Micrografting techniques for testing long-distance signalling in *Arabidopsis*. *Plant J.* 32: 255–262.

Tuskan, G.A., Difazio, S., Jansson, S., Bohlmann, J., Grigoriev, I., Hellsten, U., et al. (2006) The genome of black cottonwood, *Populus trichocarpa* (Torr. & Gray). *Science* 313: 1596–1604.

Umehara, M., Hanada, A., Yoshida, S., Akiyama, K., Arite, T., Takeda-Kamiya, N., et al. (2008) Inhibition of shoot branching by new terpenoid plant hormones. *Nature* 455: 195–200.

Wang, Y. and Bouwmeester, H.J. (2018) Structural diversity in the strigolactones. *J. Exp. Bot.* 69: 2219–2230.

Wang, Y. and Li, J. (2006) Genes controlling plant architecture. *Curr. Opin. Biotechnol.* 17: 123–129.

Wang, Y. and Li, J. (2011) Branching in rice. *Curr. Opin. Plant Biol.* 14: 94–99.

Waters, M.T., Gutjahr, C., Bennett, T. and Nelson, D.C. (2017) Strigolactone signaling and evolution. *Annu. Rev. Plant Biol.* 68: 291–322.

Wu, R. and Stettler, R. (1998) Quantitative genetics of growth and development in *Populus*. III. Phenotypic plasticity of crown structure and function. *Heredity* 81: 299–310.

Xie, X. (2016) Structural diversity of strigolactones and their distribution in the plant kingdom. *J. Pestic. Sci.* 41: 175–180.

Xie, X., Kisugi, T., Yoneyama, K., Nomura, T., Akiyama, K., Uchida, K., et al. (2017) Methyl zealactonoate, a novel germination stimulant for root parasitic weeds produced by maize. *J. Pestic. Sci*. 42: 58–61.

Xie, X., Yoneyama, K., Kisugi, T., Nomura, T., Akiyama, K., Asami, T., et al. (2015) Strigolactones are transported from roots to shoots, although not through the xylem. *J. Pestic. Sci*. 40: 214–216.

Yamada, Y., Furusawa, S., Nagasaka, S., Shimomura, K., Yamaguchi, S. and Umehara, M. (2014) Strigolactone signaling regulates rice leaf senescence in response to a phosphate deficiency. *Planta* 240: 399–408.

Yao, R., Chen, L. and Xie, D. (2018) Irreversible strigolactone recognition: a non-canonical mechanism for hormone perception. *Curr. Opin. Plant Biol*. 45: 155–161.

Yao, R., Ming, Z., Yan, L., Li, S., Wang, F., Ma, S., et al. (2016) DWARF14 is a non-canonical hormone receptor for strigolactone. *Nature* 536: 469–473.

Yoneyama, K., Xie, X., Yoneyama, K., Kisugi, T., Nomura, T., Nakatani, Y., et al. (2018) Which are the major players, canonical or non-canonical strigolactones?. *J. Exp. Bot.* 69: 2231–2239.

Yoneyama, K., Yoneyama, K., Takeuchi, Y. and Sekimoto, H. (2007) Phosphorus deficiency in red clover promotes exudation of orobanchol, the signal for mycorrhizal symbionts and germination stimulant for root parasites. *Planta* 225: 1031–1038.

Zhang, Y., Van Dijk, A.D., Scaffidi, A., Flematti, G.R., Hofmann, M., Charnikhova, T., et al. (2014) Rice cytochrome P450 MAX1 homologs catalyze distinct steps in strigolactone biosynthesis. *Nat. Chem. Biol.* 10: 1028–1033.

Zhao, L.-H., Zhou, X.E., Yi, W., Wu, Z., Liu, Y., Kang, Y., et al. (2015) Destabilization of strigolactone receptor DWARF14 by binding of ligand and E3-ligase signaling effector DWARF3. *Cell Res.* 25: 1219–1236.

Zheng, K., Wang, X., Weighill, D.A., Guo, H.-B., Xie, M., Yang, Y., et al. (2016) Characterization of *DWARF14* genes in *Populus*. *Sci. Rep.* 6: 21593.

Zhou, F., Lin, Q., Zhu, L., Ren, Y., Zhou, K., Shabek, N., et al. (2013) D14–SCF D3-dependent degradation of D53 regulates strigolactone signalling. *Nature* 504: 406–410.

Zwanenburg, B. and Blanco-Ania, D. (2018) Strigolactones: new plant hormones in the spotlight. *J. Exp. Bot.* 69: 2205–2218.

Zwanenburg, B., Mwakaboko, A.S., Reizelman, A., Anilkumar, G. and Sethumadhavan, D. (2009) Structure and function of natural and synthetic signalling molecules in parasitic weed germination. *Pest Manag. Sci*. 65: 478–491.